Solid State Ionics 180 (2009) 843–847

Contents lists available at ScienceDirect

Solid State Ionics

journal homepage: www.elsevier.com/locate/ssi

Impedance study of $SrTi_{1-x}Fe_xO_{3-\delta}$ (x = 0.05 to 0.80) mixed ionic-electronic conducting model cathode

WooChul Jung *, Harry L. Tuller

Department of Materials Science and Engineering, Massachusetts Institute of Technology, Cambridge, Massachusetts 02139 USA

ARTICLE INFO

Article history:
Received 20 September 2008
Received in revised form 13 January 2009
Accepted 1 February 2009

Keywords:
SOFC cathode
Mixed conductor
Surface oxygen exchange
Impedance spectroscopy
Thin film

ABSTRACT

$SrTi_{1-x}Fe_xO_{3-\delta}$ (STF) model cathodes, with compositions of x = 0.05 to 0.80 were deposited onto single crystal yttria stabilized zirconia by pulsed layer deposition as dense films with well defined area and thickness and studied by electrochemical impedance spectroscopy as a function of electrode geometry, temperature and pO_2. The STF cathode was observed to exhibit typical mixed ionic-electronic behavior with the electrode reaction occurring over the full electrode surface area rather than being limited to the triple phase boundary. The electrode impedance was observed to be independent of electrode thickness and to the introduction of CGO interlayers and inversely proportional to the square of the electrode diameter, pointing to surface exchange limited kinetics. Values for the surface exchange coefficient, *k*, were calculated and found to be comparable in magnitude to those exhibited by other popular mixed ionic-electronic conductors such as (La,Sr)(Co,Fe)O_3, thereby, confirming the suitability of STF as a model mixed conducting cathode material. The surface exchange coefficient, *k*, was also found to be insensitive to orders of magnitude change in both bulk electronic and ionic conductivities.

1. Introduction

Progress in achieving improved solid oxide fuel cell (SOFC) performance, particularly at reduced temperatures, has been constrained, in part, by an inadequate understanding of the kinetic processes controlling cathode performance and the resultant inability to further reduce cathode polarization losses. The perovskite materials system, $SrTi_{1-x}Fe_xO_{3-\delta}$ (STF), was recently shown to exhibit promising electrode properties when applied to yttria stabilized zirconia electrolytes while serving as a model mixed ionic electronic conducting (MIEC) cathode [1]. STF is a continuous solid solution between strontium titanate ($SrTiO_3$) and strontium ferrite ($SrFeO_3$) [2]. Strontium titanate is a wide-band-gap semiconductor ($E_g^o = 3.2$ eV at T = 0 K) with rather low conductivity in the undoped state [3] while substitution of Fe for Ti, results in a systematic decrease in band gap and an increase in electron, hole and oxygen vacancy density, providing in turn, mixed conductivity with high levels of electronic and ionic conductivities [4]. From the perspective of this study, the most important advantage of STF as a model cathode material is the ability to control both the magnitude and ratio of electronic and ionic conductivity as well as its stability over a wide range of pO_2 and temperature. For similar reasons, the potential of STF (x = 0.4) as an anode was previously investigated [5].

In previous work by the authors, thin film STF model cathodes, with compositions x = 0.35 and 0.50, prepared with well defined area and thickness by pulsed layer deposition (PLD) were investigated by electrochemical impedance spectroscopy (EIS) as a function of electrode geometry, temperature and oxygen partial pressure [1]. The STF cathodes were observed to exhibit typical mixed ionic-electronic behavior with the electrode reaction occurring over the full electrode surface area rather than being limited to the triple phase boundary. Based on insensitivity of the electrode impedance to electrode thickness and to the insertion of a $Ce_{0.9}Gd_{0.1}O_{2-\delta}$ (CGO) interlayer between the STF electrode and YSZ electrolyte, the rate limiting process was assigned to surface oxygen exchange kinetics. Calculated values for the surface exchange coefficient, *k*, were found to be comparable in magnitude to those exhibited by other popular mixed ionic-electronic conductors such as $La_{0.6}Sr_{0.4}Co_{0.2}Fe_{0.8}O_3$ (LSCF), in spite of the fact that the electronic conductivity of STF was several orders of magnitude lower than that of the other popular mixed conductors.

In the present contribution, the Fe percentage has been significantly extended to both low and high fractions of Fe substitution for Ti (x = 0.05 to 0.80) to aid in obtaining an improved understanding of the correlation between electrochemical performance and materials parameters. By taking advantage of the simplified and well-defined electrode geometry, the impedance governing processes are confirmed and the observed trends are discussed in relation to the known defect and transport properties of STF.

2. Experimental

STF thin films were prepared by means of pulsed laser deposition (PLD) from oxide targets of the respective materials and deposited onto (100) oriented single crystal yttria doped zirconia (YSZ) substrates

* Corresponding author.
E-mail address: wcjung@mit.edu (W. Jung).

0167-2738/$ – see front matter © 2009 Elsevier B.V. All rights reserved.
doi:10.1016/j.ssi.2009.02.008

($10\times10\times0.5$ mm^3 and $15\times15\times0.5$ mm^3, MTI Corporation, Richmond, CA). Detailed information regarding oxide target preparation and PLD deposition conditions can be found in the previous study [1]. In some cases, a ~50 nm thick interlayer of $Ce_{0.9}Gd_{0.1}O_{2-\delta}$ was deposited between the YSZ electrolyte and the STF electrode by reactive RF sputtering from an oxide target.

The resulting polycrystalline films exhibited the perovskite structure with highly (110) orientated texture as confirmed by X-ray diffraction (Rigaku RU300). Grain sizes of between 100 and 200 nm and surface roughness of ~2 nm were measured by atomic force microscopy (Digital Instruments Nanoscope IIIa) while film thicknesses ranging from 70 to 440 nm were determined by surface profilometry (Tencor P-10).

A symmetrical structure with identically sized (9 mm × 9 mm) STF electrodes on both sides of the YSZ electrolyte was used for EIS measurements as shown in Fig. 1. Au mesh and Au paste were placed on each STF electrode surface, serving as current collector. Both a custom-designed enclosed probe station, manufactured by McAllister Technical Services (Coeur d'Alene, ID) and a tube furnace were used for the EIS measurements at temperatures between 570 °C and 650 °C and at oxygen partial pressure range between 2×10^{-5} atm and 1 atm. EIS measurements, covering the frequency range from 7 mHz to 1 MHz with an amplitude of 20 mV were performed with a Solarton 1260 or 1250 impedance analyzer operated in combination with a Solartron 1286 potentiostat.

3. Results

Fig. 2 shows typical impedance results obtained for the symmetrical structure in which the STF electrodes were of composition x = 0.05 or 0.35, designated as STF5 or STF35, respectively. For most values of x (0.10, 0.35, 0.50, and 0.80), the spectra exhibit an offset resistance (R_{off}) followed by a nearly ideal semicircle at low frequencies (LF), which are attributed to the ohmic resistance of the YSZ electrolyte and the electrode impedance of the STF electrode, respectively. While there is evidence for a very small semicircle at high frequencies at some temperatures, it is very difficult to deconvolute from the much larger semicircle at lower frequencies. When one attempts to do so, no systematic value for the equivalent circuit elements can be derived for the different temperatures and oxygen partial pressures. Furthermore, evident inductive contributions may confuse the interpretation further. As a consequence, no further attempts are made to interpret this small feature. However, in the case

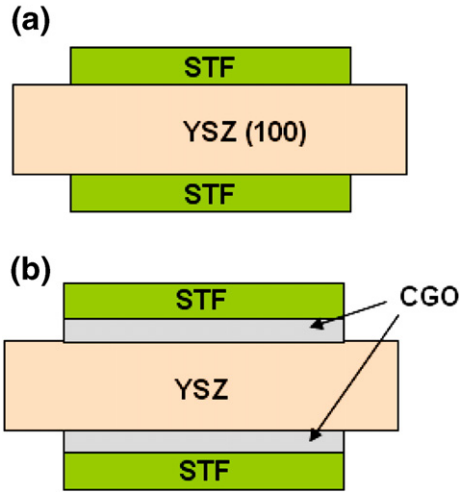

Fig. 1. Schematic illustrations of the symmetrical structures used in this work: (a) identically dimensioned STF electrodes (9 mm × 9 mm) on both sides of the YSZ electrolyte, and (b) additional CGO interlayers inserted between the STF electrode and the YSZ electrolyte.

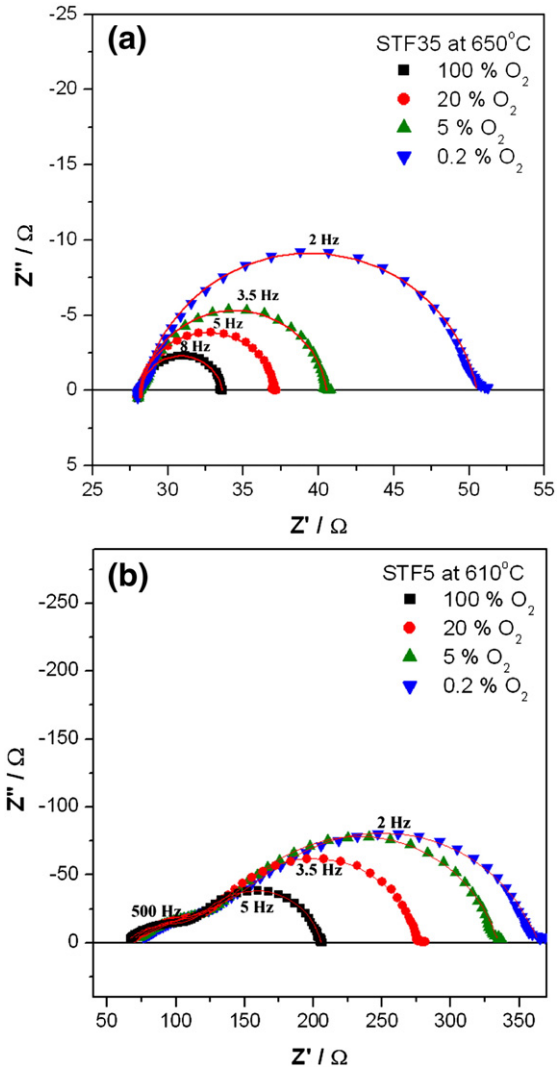

Fig. 2. Typical impedance spectroscopy plots of (a) STF35 at T = 650 °C, (b) STF5 at T = 610 °C, at various oxygen partial pressures.

of STF5, a clear distorted semicircle, located at higher frequencies (HF), in between the offset resistance and the nearly ideal semicircle, is obtained and is also attributed to the STF electrode. Therefore, the authors assumed the high frequency feature for a Fe fraction higher than 5 mol% is insignificant within measurement error. For a more detailed discussion of the impedance spectra analysis of these thin film structures, the reader is referred to the previous publication by the authors [1].

Given the near ideal semicircular shape of the spectra at low-frequency (LF) in Fig. 2, one can assign this response to that expected from a parallel resistor–capacitor (R–C) circuit. For this work, the capacitor is replaced by a more general constant phase element (CPE), for which the impedance is given by

$$Z = \frac{1}{Q(i\omega)^n} \tag{1}$$

where Q and n are empirical constants; for further information of the CPE, the reader is referred to [6,7].

Applying the expression for a true capacitance according to [8], one obtains

$$C = Q\omega_{max}^{n-1} = \left(R^{1-n}Q\right)^{1/n}. \tag{2}$$

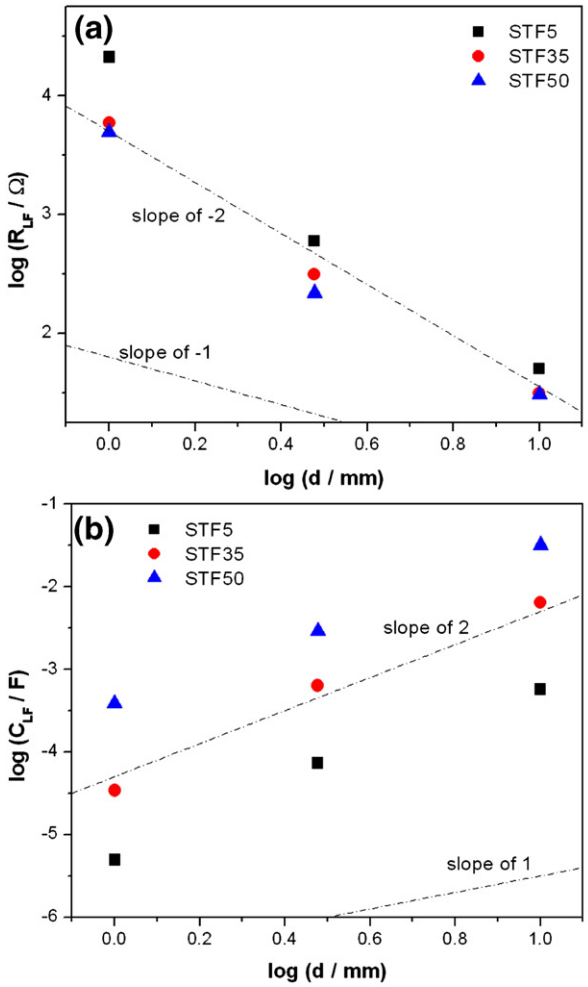

Fig. 3. Double-logarithmic plots of R_{LF} and C_{LF} vs. diameter measured for STF electrodes: 5, 35, and 50 Fe mol% at 590 °C in air.

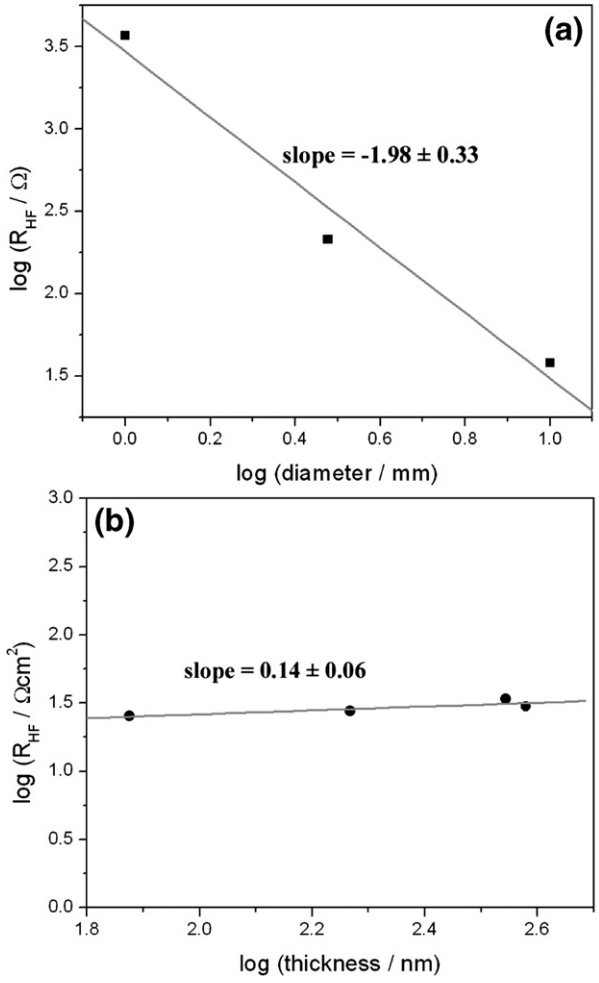

Fig. 5. Double-logarithmic plots of R_{HF} vs. (a) diameter and (b) thickness, measured for STF5 in air at 590 °C and 610 °C, respectively.

The R and C values derived from the ideal LF spectra are designated as R_{LF} and C_{LF}, while those from the distorted HF spectra in STF5 are called R_{HF} and C_{HF}, respectively. From the data, one derives, for example, a C_{LF} value at 650 °C of approximately 12 mF/cm^2 for a 160 nm thick STF50 film, consistent with that expected for a chemical capacitance [1]. In the following, the geometrical and temperature dependences of these parameters are examined.

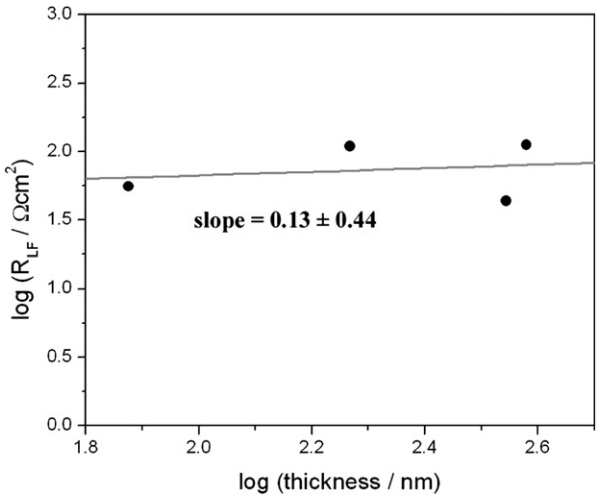

Fig. 4. Double-logarithmic plots of R_{LF} vs. electrode thickness, measured for STF5 in air at 610 °C.

Log R_{LF}, plotted vs log electrode diameter (Fig. 3a) for STF5, 35, and 50, shows a power law dependence of ~−2 regardless of Fe composition while the corresponding plot of log C_{LF} vs log electrode diameter (Fig. 3b) demonstrates instead a power law dependence of ~+2. Log R_{LF} vs log electrode thickness is also plotted in Fig. 4, providing a power law dependence of 0.13 ± 0.44. Plots of log R_{HF} vs electrode diameter and thickness for STF5, show power law dependences of -1.98 ± 0.33 and 0.14 ± 0.06, respectively (see Fig. 5).

Table 1 records the activation energies (E_a) derived from an examination of the Arrhenius dependence of R_{LF} on temperature for the various STF compositions. E_a is observed to generally decrease with increasing iron fraction ranging from 2.5 eV for STF5 to 1.9 eV at STF80. Fig. 6 compares the impedance spectra of STF5 measured in air at 580 °C with and without the CGO layer between the YSZ electrolyte and the STF electrode. The resistance values differ by ~10%, indicating

Table 1
Activation energies for STF samples with different Fe mol% obtained from impedance measurements in the temperature range 570–650 °C in air.

Fe mol%	Ea/eV
5	2.54 ± 0.09
10	2.21 ± 0.07
35	2.00 ± 0.16
50	1.80 ± 0.14
80	1.90 ± 0.12

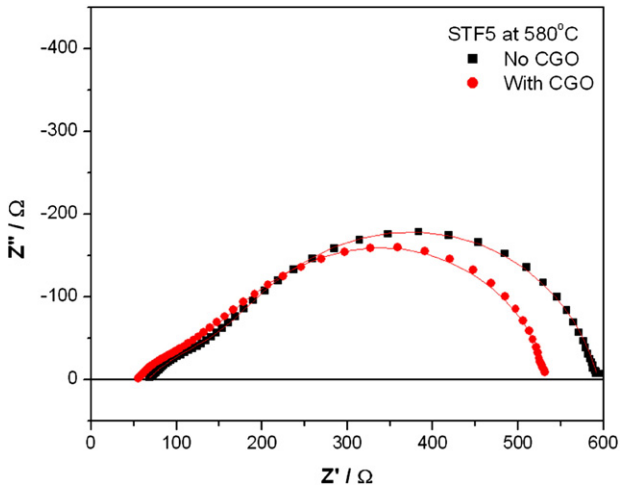

Fig. 6. Comparison of two impedance spectra, one measured for STF5 (a) without a CGO interlayer and (b) with a CGO interlayer at 580 °C in air. The results suggest that the interfacial CGO layer has little impact on electrode performance.

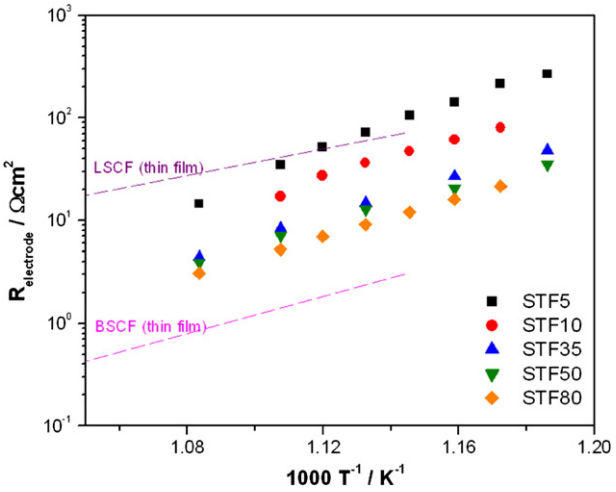

Fig. 7. Temperature dependence of Area Specific Resistance (ASR) for STF (solid dots), and for other dense thin film MIEC electrodes (LSCF and BSCF) fabricated by PLD (dashed lines), the latter obtained from the work of Baumann, et al from Ref [9].

that the interfacial CGO layer has, at most, a minor impact on electrode performance.

4. Discussion

Oxygen reduction can take place either at the triple phase boundary (TPB) between electrode, electrolyte and gas phase or, for a dense mixed ionic electronic conductor (MIEC) electrode, at the surface of the electrode corresponding to the double phase boundary between electrode and gas phase. The use of dense thin film electrodes with simple geometry enables one to obtain a quantitative relationship between electrode impedance and geometry. In the earlier study on STF35 and STF50, the oxygen surface exchange kinetics were found to be limiting [1]. The results of this study, covering a much broader composition range (STF5-STF80), are consistent with these conclusions. The power dependence observed for STF5 was -2.62 ± 0.34, while it was -2.20 ± 0.35 and -2.27 ± 0.22 for STF50 and STF35, respectively. A power law dependence of approximately -2 (rather than -1) for the dependence of both log R_{LF} and log R_{HF} on log electrode diameter (1–10 mm) (see Figs. 3 and 5a) confirms that the electrode resistances are inversely proportional to electrode surface area, rather than to the triple phase boundary length (TPBL). One can thus conclude that the oxygen reduction reaction largely occurs over the electrode surface area, rather than being limited to the TPB, as also reported for thin film LSC and LSCF MIEC electrodes [9–11]. This is concluded in spite of the relatively large error bars given that the slopes come nowhere close to unity, characteristic of TPB control.

Furthermore, the near independence of R_{LF} and R_{HF} on electrode thickness (see Figs. 4 and 5a) eliminates mass transport through the electrode as the limiting step. Finally, the insensitivity of $R_{HF} + R_{LF}$ to the insertion of the CGO interlayer between the electrolyte and the STF electrode, as shown in Fig. 6, confirms that interfacial transfer between the electrolyte and the electrode is not limiting. One therefore concludes that there is a common limiting process for nearly the full STF solid solution system ($x = 0.05$ to 0.80 studied to date) which must be attributed to the surface oxygen exchange reaction occurring at the surface of the STF electrodes.

The source of the additional HF impedance response for STF5 remains unclear. Given its distorted shape, weak pO_2 dependence, and slightly smaller activation energy (~2.2 eV), one can reasonably assume that it results from an additional process, not evident at this stage. Further investigations are planned to investigate the physical origin of the HF semicircle in STF5.

The area specific resistance (ASR) of the STF electrodes is plotted as a function of reciprocal temperature in Fig. 7. For comparison, the ASR values for dense thin films of the more typical MIEC cathodes also prepared by PLD are included. Several key points should be noted. First, there is a gradual reduction in ASR with increasing Fe fraction which appears to largely saturate for Fe levels above STF35. As discussed above, the substitution of Fe for Ti results in an increase in both electronic and ionic conductivities and a decrease in bandgap [4]. Since the ASR decreases by approximately a factor of 10 in going from STF5 to STF 80 while the ionic and electronic conductivities increase by about a factor of 1000 [4], this suggests that the surface exchange kinetics are, at best, weakly influenced by the bulk electrical properties of STF. The results also suggest that little is likely to be gained with respect to cathode performance by increasing the Fe level above 35 mol%. A lower Fe fraction is likely to be advantageous with respect to reduced chemical expansion coefficient and chemical stability against aging due to order-disorder transitions.

The ASR values for thin film STF electrodes are comparable to that of thin film $La_{0.6}Sr_{0.4}Co_{0.2}Fe_{0.8}O_3$, a commonly used MIEC cathode material. The roughly 2 eV values for E_a reported for STF in Table 1 are close to those reported for (Ba,Sr)(Co,Fe)O_3 (BSCF) and (La,Sr)FeO_3 (LSF) (1.8 eV), but higher than those reported for LSC and LSCF (1.3–1.6 eV) [9]. Because of STF's relatively high activation energy, even STF5 exhibits a smaller ASR than LSCF at temperature above 600 °C. This indicates the suitability of STF as a realistic mixed conducting model cathode material.

Given conclusions regarding the rate limiting step in STF, the surface oxygen exchange coefficient can be extracted from the electrode resistance by [12];

$$k^q = \frac{kT}{4e^2 R_s c_o} \tag{3}$$

(k: Boltzmann constant, e: electron charge, T: temperature, R_s: area specific resistance and c_o: total concentration of lattice oxygen with the value 4.92×10^{22} cm^{-3} used in this calculation [4].).

Table 2
Surface exchange coefficient (k), electronic (σ_{el}) and ionic (σ_{ion}) conductivity, and electronic transfer number at 800 °C for $SrTi_{1-x}Fe_xO_3$ ($x = 5$, 10, 35, and 50) and $La_{0.6}Sr_{0.4}Co_{0.2}Fe_{0.8}O_3$ [14,15].

800 °C	k/cm s^{-1}	σ_{el}	σ_{ion}	t_{el}
STF5	1.2×10^{-5}	4.5×10^{-3}	5.7×10^{-4}	0.88681
STF10	1.4×10^{-5}	1.4×10^{-2}	1.7×10^{-3}	0.89059
STF35	2.0×10^{-5}	9.9×10^{-1}	3.5×10^{-2}	0.96635
STF50	1.7×10^{-5}	1.8	3.6×10^{-2}	0.97999
$La_{0.6}Sr_{0.4}Co_{0.2}Fe_{0.8}O_3$	5.6×10^{-6}	3.0×10^{2}	8.0×10^{-3}	0.99997

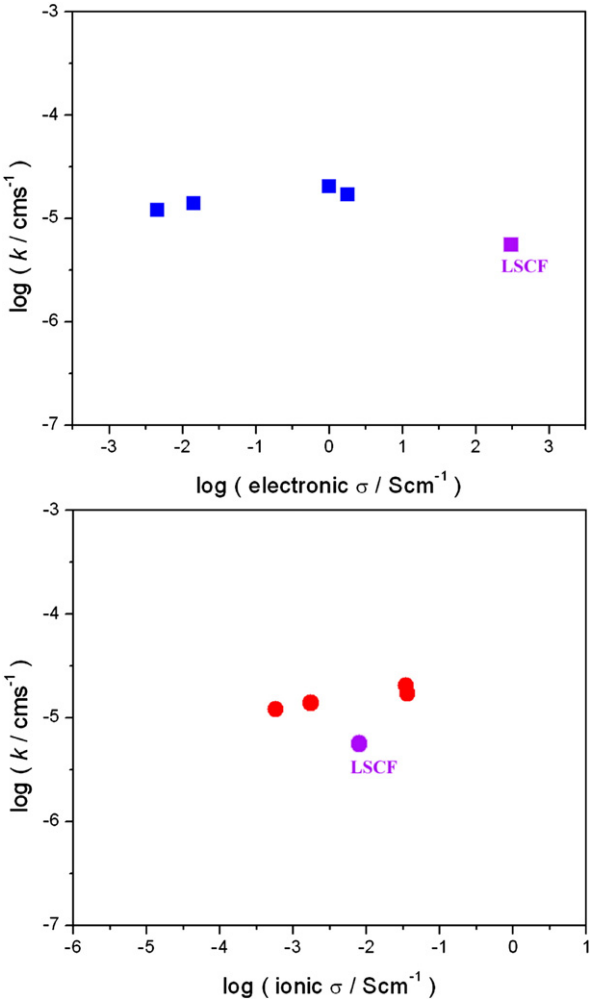

Fig. 8. Double-logarithmic plots of k vs. σ_{el} and σ_{ion} for STF and LSCF cathodes [14,15] at 800 °C. k values for STF were calculated from the EIS measurements and extrapolated at 800 °C.

Calculated k^q values, averaged from more than three different samples and extrapolated to 800 °C, are shown in Table 2. The calculated STF surface oxygen exchange coefficients are again comparable in magnitude to those reported for bulk LSCF. This is perhaps surprising given that the electronic conductivity of the STF cathodes is several hundred times lower than those of LSCF at 800 °C. An electronic conductivity of only 4.5×10^{-3} (S/cm) at 800 °C for STF5 is enough to obtain comparable high surface exchange kinetics ($k^q = 1.2\times10^{-5}$ cm/s at 800 °C).

In Fig. 8, σ_{el} and σ_{ion} values obtained for bulk STF samples, with a range of Fe levels [4], are plotted vs k^q. The Surface exchange kinetics, in fact, exhibit a very weak dependence on both σ_{el} and σ_{ion} with respective power law dependences of 0.07 ± 0.02 and 0.11 ± 0.02 respectively. Surprisingly, k^q maintains nearly the same magnitude over nearly five orders of magnitude change in σ_{el} when data for LSCF is also included (see Fig. 8). It is normally assumed that that both high σ_{el} and σ_{ion} guarantee fast surface exchange reactions, although available kinetic and transport data remain limited and the relative roles of σ_{el} and σ_{ion} are not clearly established. However, based on these results, it is reasonable to conclude that σ_{el}, at least above a certain minimum magnitude, does not play the limiting role in the surface exchange reactions according to the Fig. 8. The same can be said about the magnitude of the ionic conductivity, although our data is more limited in extent.

Before generalizing these conclusions, one should note that the magnitudes of the ionic and electronic conductivities used in this study were measured for bulk polycrystalline STF specimens [4]. There is evidence that the electrical properties of thin film cathodes can differ considerably, in some cases, from those of bulk specimens [13]. This is all the more possible for the few atomic layers adjacent to the surface, to which the surface exchange reactions are likely highly sensitive. Studies of the electrical properties of thin film STF and a more intimate characterization of their surfaces are underway and should help to further clarify these issues.

5. Conclusions

The cathodic behavior of thin film STF on YSZ was systematically investigated over a wide Fe fraction and the electrode impedance was found to be largely controlled by surface oxygen exchange kinetics. STF showed surprisingly low area specific resistance (ASR) between 570 °C and 650 °C with surface exchange coefficient values, k, comparable in magnitude to those exhibited by other popular mixed conductors such as LSC and LSCF, thereby, confirming its suitability as a model MIEC cathode material. Surprisingly, k was found to maintain nearly the same magnitude even when the bulk electronic and ionic conductivities varied by many orders of magnitude (over nearly five orders of magnitude change in σ_{el}). Studies of the electrical properties of thin film STF and a more intimate characterization of their surfaces are underway and to further clarify these observations.

Acknowledgments

This work was supported by the National Science Foundation material world network collaboration under grant number DMR-0243993 and originally initiated by the Department of Energy under grant number DE-FC26-05NT42624. This work made use of the Shared Experimental Facilities supported by the MRSEC Program of the National Science Foundation under grant number DMR 02-13282. The authors thank Prof. E. Ivers-Tiffée's group, Univ. Karlsruhe and Dr. A. Rothschild, Technion for providing detailed STF defect chemical data and constructive discussion, and Prof. Caroline A. Ross's group, MIT for use of the PLD system. The authors also thank the Samsung Scholarship for financial support.

References

[1] W. Jung, H.L. Tuller, Journal of The Electrochemical Society 155 (2008) B1194.
[2] L.H. Brixner, Materials Research Bulletin 3 (1968) 299.
[3] G.M. Choi, H.L. Tuller, D. Goldschmidt, Physical Review B 34 (1986) 6972.
[4] A. Rothschild, W. Menesklou, H.L. Tuller, E. Ivers-Tiffée, Chemistry of Materials 18 (2006) 3651.
[5] D.P. Fagg, V.V. Kharton, A.V. Kovalevsky, A.P. Viskup, E.N. Naumovich, J.R. Frade, Journal of the European Ceramic Society 21 (2001) 1831.
[6] E. Barsoukov, J.R. Macdonald, Impedance Spectroscopy-Theory, Experiment, and Applications, John Wiley & Sons, Hoboken, New Jersey, 2005 Chap 2.1.2.3.
[7] D.D. Macdonald, Electrochimica Acta 51 (2006) 1376.
[8] J. Fleig, Solid State Ionics 150 (2002) 181.
[9] F.S. Baumann, J. Fleig, G. Cristiani, B. Stuhlhofer, H.U. Habermeier, J. Maier, Journal of the Electrochemical Society 154 (2007) B931.
[10] F.S. Baumann, J. Fleig, H.U. Habermeier, J. Maier, Solid State Ionics 177 (2006) 1071.
[11] J. Fleig, Journal of Power Sources 105 (2002) 228.
[12] J. Maier, Physical Chemistry of Ionic Materials, John Wiley & Sons, Chichester, England, 2004.
[13] A. Bieberle-Hutter, M. Sogaard, H.L. Tuller, Solid State Ionics 177 (2006) 1969.
[14] S.J. Benson, R.J. Chater, J.A. Kilner, Proceedings of the 3rd International Symposium on Ionic and Mixed Conducting Ceramics (Electrochemical Society Proceedings Series), Paris, France, PV 97-24, 1997, p. 596.
[15] H. Ullmann, N. Trofimenko, F. Tietz, D. Stöver, A. Ahmad-Khanlou, Solid State Ionics 138 (1-2) (2000) 79.